Nano World Journal

https://doi.org/10.17756/nwj.2023-119

Research Article

Open Access

Comparative Analysis of Thermal Behavior of Coagulation-processed Nanocomposites: Polypropylene and Polyamide-6

Zaib Un Nisa[1*], Lee Kean Chuan[1], Beh Hoe Guan[1], Faiz Ahmad[2] and Saba Ayub[1]

[1]*Department of Fundamental and Applied Sciences, Universiti Teknologi PETRONAS, Seri Iskandar Perak, Malaysia*
[2]*Department of Mechanical Engineering, Universiti Teknologi PETRONAS, Seri Iskandar Perak, Malaysia*

[*]Correspondence to:
Zaib Un Nisa
Department of Fundamental and Applied Sciences,
Universiti Teknologi PETRONAS,
Seri Iskandar Perak, Malaysia.
E-mail: zaib_20001001@utp.edu.my

Received: June 28, 2023
Accepted: August 04, 2023
Published: August 11, 2023

Citation: Nisa ZU, Chuan LK, Guan BH, Ahmed F, Ayub S. 2023. Comparative Analysis of Thermal Behavior of Coagulation-processed Nanocomposites: Polypropylene and Polyamide-6. *NanoWorld J* 9(3): 71-76.

Published by United Scientific Group

Abstract

Black nanocarbon developed from bamboo (*Gigantochloa scortechinii*) was utilized as reinforcement for two thermoplastic polymers. The nanocomposites of polypropylene (PP) and polyamide-6 (PA-6) were synthesized by applying a coagulation scheme. Methanol was used as a coagulant for the nanocomposite preparation. Comparative analysis was accomplished with three percent filler mixing. Structural interpretation of the nanocomposite was carried out using Fourier-transform infrared (FTIR) spectroscopy. The investigation of the thermal and melting behavior of the nanocomposites was performed using thermogravimetric analysis (TGA) and differential scanning calorimetry (DSC) techniques. The obtained results of the respective nanocomposite were interrelated to the neat PP and PA-6. A comparative investigation was done on the effective role of filler in each of the two polymers. The thermal analysis revealed that nanocomposites were stable at higher weight loss temperatures compared with their neat composites. The two nanocomposites presented a different change in thermal properties with the same amount of the filler. DSC analysis disclosed the lowering in heat of melting of the coagulation processed products.

Keywords

Synthesis, Nanocomposite, Nanocarbon, Thermoplastic polymers, Polypropylene, Coagulation

Introduction

The carbon products with high surface area and porous morphology are universal and ubiquitous in modern-day technical research and scientific development [1, 2]. Activated carbon-based materials have presented remarkable consideration and exhibited fantastic aptitudes in many disciplines. This owed to exceptional properties including elevated surface area, variable pore size, range of monodispersed outer pore space, different pore shapes, uniform nanosized frameworks, variable particle sizes, and abundant compositions [3].

The insidious applications of carbons product are recognized due to their incredible physicochemical characteristics, including advancing the hydrophobicity of the surfaces, superior corrosion endurance, great thermal constancy, improved surface area, good mechanical permanence, easy treatment, and little manufacturing cost [4]. Carbon black has enticed valuable consideration for its favorable applications in numerous fields concerning catalyst support, adsorption and isolation of bulky biomolecules, electrical devices with double-layer capacitors, purification of wastewater, and air treatment plants [5]..

Biomass products have been manufactured and obtained valuable interest as active electrode material and supercapacitor applications [6]. The raw carbona-

ceous biomaterial is transformed into activated black carbon/char [7]. The intended use of the subsequent product is dependent on the treatment path for activation and selection of the raw material. In common, the shrinkage of the cellulose precursor takes place during carbonization which plays a significant role in the property development of the end product [8, 9].

Carbon products are usually synthesized in an economic way employing the carbonization of agricultural waste. The lignocellulosic waste material of fruit stones, twigs, and shells have demonstrated to be exceptional for the fabrication of activated carbons materials because of their high-level carbon content, smaller inorganic contaminations, and adequate hardness [10, 11]. There is widespread use of bio-based fillers in polymers for aerospace devices, electronic and conductive applications, chemical modifications, heavy metal purification treatment, filters, and absorbents [12, 13].

Biobased thermoplastic polymer composites are routinely fabricated. PP and PA-6 are practical thermoplastics due to their superior wear resistance, excellent coefficient of friction, and extremely good temperature resistance and impact properties [14, 15]. They are utilized in surface protection, fittings, connectors, and cable protection systems [16]. These thermoplastics possess low density, enduring strength, mechanical properties, and heat resistance, due to which they are extensively employed in industries like aircraft, automotive parts, and aerospace [17, 18].

The physical properties of thermoplastics can be improved by the addition of organic and inorganic nano-filler during composite formation [19]. The effective use of many thermoplastic polymers has been hampered due to their inadequacies in thermal stability and flame-resistant properties [20]. These properties owe considerable interest and modification in properties is achieved by the introduction of nanofillers via composite formation [21, 22]. Composite fabrication modifies the substrate by the creation of physical interaction with the polymer matrix [23].

In the current work activated carbon black obtained from the bamboo plant was used as filler in two industrial thermoplastic polymers. Considering nanocomposite fabrication a useful approach the research was focused on nanocomposite synthesis using the coagulation method. The research was focused to explore the thermal, spectroscopic, and melting properties of the nanocomposites synthesized with carbon black of the bamboo plant. Comparative changes were investigated at fixed loading of filler and an assessment of thermal and melting behavior was made with the neat polymer.

Experimental

Materials and reagents

PP powder (Molecular weight ¼ 28.9 x 10^4 g mol^{-1}, polydispersity = 3.45, isotactic) was purchased from ABV Global Holdings Sdn Bhd, PA-6 pellets were obtained from Sigma Aldrich (density = 1.084 g/ml at 25 °C). Dimethyl sulfoxide (DMSO) Extra pure SLR was supplied by Fischer Scientific (b.p. = 189 °C), Xylene reagent grade (b.p. = 137 - 140 °C), and methanol was obtained from Sigma-Aldrich (b.p. = 64 °C) and used as received. The black nanocarbon (CB) of the bamboo plant was received from Future Food, Japan with 3000 super tiny mesh sizes.

Preparation of CB@nanocomposite

CB@PP and CB@PA-6 nanocomposites synthesized using the coagulation technique are presented in figure 1. 0.97 g of PP was dissolved in 50 ml xylene using a hot plate at 120 °C for 30 minutes. Similarly, 0.97 g of PA-6 was dissolved in DMSO at 270 °C utilizing a hot plate. 0.03 g of CB was separately mixed in two solvents i.e., DMSO and xylene. The filler was homogeneously mixed in the solvents for 30 minutes using ultrasonication to get homogeneous dispersion. The two polymeric solutions were mixed with respective filler dispersion using ultrasonication for another 30 minutes. 50 ml of methanol was added into both polymeric solutions with continuous mixing. After filtration, the two flocculate products were dried at 80 °C under a vacuum.

Characterization

Three characterization techniques were utilized to analyze the structural, thermal, and morphological properties of CB@PP and CB@PA-6 nanocomposites. FTIR spectra were recorded on an FTIR instrument, Perkin Elmer (FTIR Frontier) using KBr solid-state analysis. Thermal characterization was performed using Perkin Elmer (STA6000) thermobalance, at a heating rate of 10 °C/min under N_2 atmosphere up to a maximum temperature of 600 °C. DSC analysis test was performed under N_2 using Perkin Elmer (Pyris-1) instrument.

Figure 1: Samples **(a)** PP, **(b)** PA-6, **(c)** CB@PP, and **(d)** CB@PA-6.

The samples were heated from 50 - 400 °C at a heating rate of 10 °C/ min.

Results and Discussion

FTIR analysis of the samples

CB@PP and CB@PA-6 nanocomposites were synthesized using the coagulation technique. An investigation of spectroscopic analysis was done using FTIR characterization. The results of FTIR spectra obtained from 4000 - 500 cm^{-1} on the instrument are given in table 1 and table 2, respectively. The obtained spectra are given in figure 2.

In the spectra, of CB@PP peaks of C-H aliphatic stretch were very sharp and observed at 2906 cm^{-1} and 2849 cm^{-1}. These peaks are assigned to asymmetric and symmetric vibrations of the C-H bond. The characteristic peak for -CH_2- bending vibrations is present at 1468 cm^{-1}. In the fingerprint region, two peaks were observed for the rocking vibration of methylene bonds. One present at 713 cm^{-1} was assigned to the crystalline nature and the other one at 569 cm^{-1} was attributed to the amorphous character of the substrate.

CB@PA-6 presented representative peaks in fingerprint and functional group regions. The peak due to the amidic N-H bond was very intense and present at 3425 cm^{-1}. The methylene stretching vibration was observed at 2930 cm^{-1} in the functional group region and the corresponding bending vibration was present at 1264 cm^{-1}. The carbonyl moiety of the amide group presented its characteristic peak at 1642 cm^{-1} with medium intensity. The carbon atoms attached to the C=O bond have an absorption at 1023 cm^{-1}. The C-N functionality exhibited its distinctive peak at 1539 cm^{-1}.

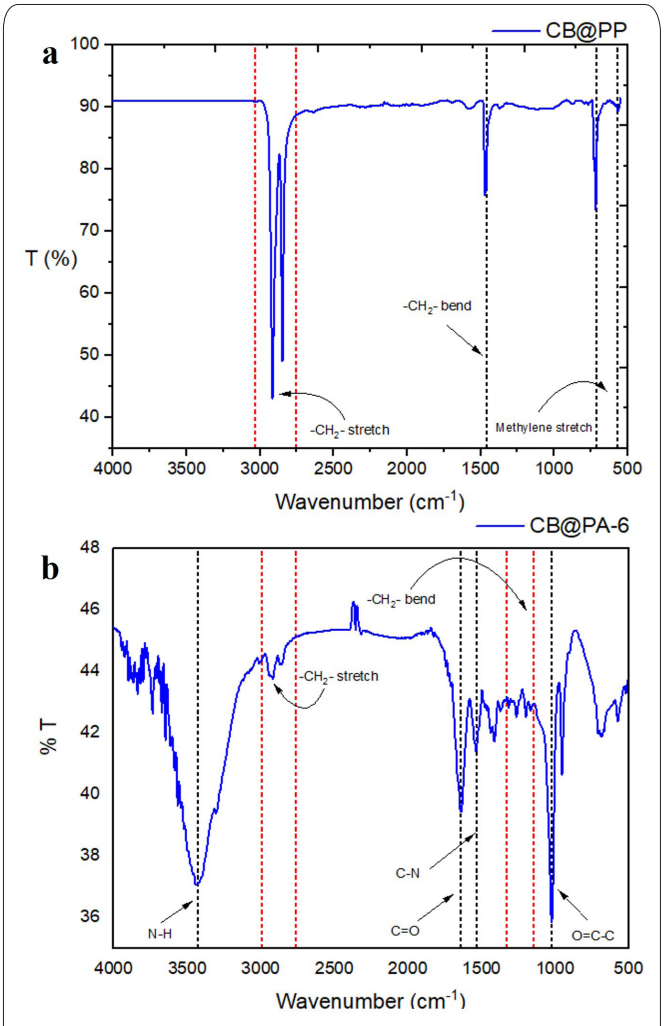

Figure 2: FTIR spectra of **(a)** CB@PP and **(b)** CB@PA-6.

Thermal analysis of samples

Figure 3 presents TGA thermograms of coagulation-processed nanocomposites under N_2 atmosphere. The detailed data are elaborated in table 3. The thermal stability of the synthesized nanocomposite was assessed in terms of observed temperature at different weight loss i.e., 5 % weight loss (T_5), 10% weight loss (T_{10}), final degradation (T_f), and residual weight at T_f (R_f). The comparison of each nanocomposite was made with the neat thermoplastic polymer.

It was revealed that adding the same percentage of the CB of the bamboo plant has shown different trends in thermal stability. Using three percent filler loading the thermal stability of CB@PP has increased compared with neat polymer however adding the same content to the PA-6 polymer shows an anomalous trend. All the neat and nanocomposite samples were observed to be stable above 450 °C. CB@PP compared to PP presented a rise in T_5 and T_{10} of 45 °C and 15 °C, respectively. On the contrary, CB@PA-6 showed a drastic decline in initial weight loss temperature. There is a fall of 308 °C and 301 °C in T_5 and T_{10}, respectively.

This behavior revealed the fact CB filler is not playing a supportive role for PA-6 for initial degradation. It is assumed that the filler has reduced the thermal stability at initial weight

Table 1: FTIR data of CB@PP.

	Wavenumber (cm^{-1})				
Sample	**C-H (Aliph Stret)**	**C-H (Aliph Stret)**	**-CH_2- (Bend)**	**Meth (Cry, Rock)**	**Meth (Amp, Rock)**
CB@PP	2906 (s)	2849 (s)	1468 (m)	713 (m)	569 (m)

Note: Aliph = Aliphatic, Meth = Methylene, Stret = Stretching, Amp = Amorphous, Cry = Crystalline, Bend = Bending, Rock = Rocking, s = Sharp, m = Medium.

Table 2: FTIR data of CB@PA-6.

	Wavenumber (cm^{-1})					
Sample	**N-H (Stret)**	**-CH_2- (Stret)**	**C=O (Stret)**	**C-N (Stret)**	**-CH_2- (bend)**	**O=C-C**
CB@PA-6	3425 (s)	2930 (s)	1642 (m)	1539 (w)	1264 (w)	1023 (s)

Note: Stret = Stretching, Bend = Bending, Rock = Rocking, s = Sharp, m = Medium.

Table 3: TGA data of neat polymers and their nanocomposites.

Compounds	T_5 (°C)	T_{10} (°C)	T_{50} (°C)	T_f (°C)	R_f (%)
PP	347	410	460	498	2.8
CB@PP	394	420	461	590	20.6
PA-6	377	400	437	479	10.4
CB@PA-6	69	98	435	571	0.3

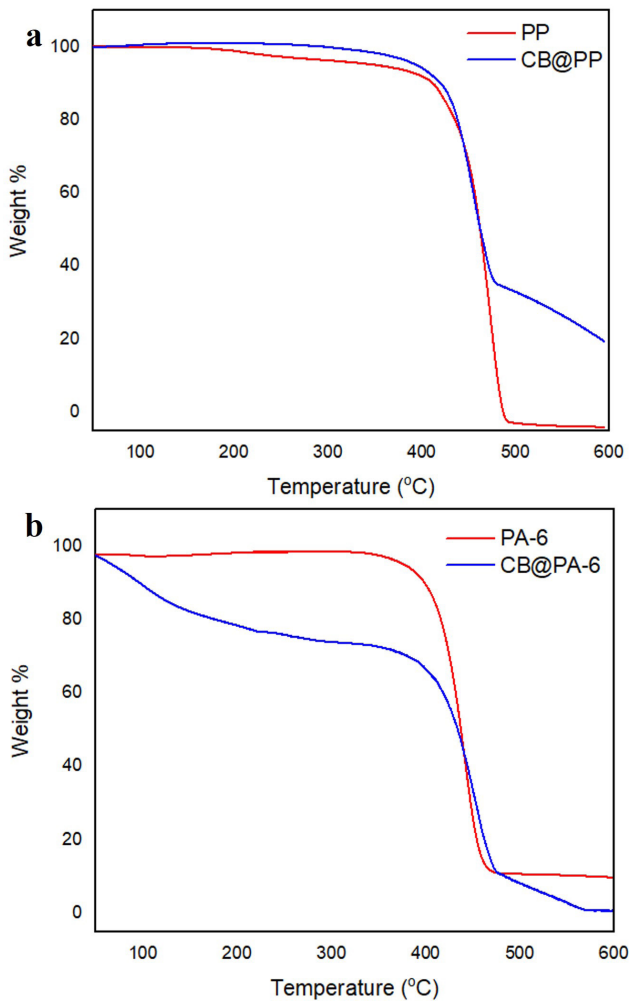

Figure 3: TGA curves of the samples **(a)** PP and CB@PP, and **(b)** PA-6 and CB@PA-6.

losses by decreasing the productive stronger hydrogen bonding presented in the neat polymer.

It was evidenced that coagulation processed CB@PP and CB@PA-6 have resented comparable values of T_{50} which lies in the range of 435 °C to 461 °C. The maximum degradation temperature (T_f) for the two synthesized nanocomposites is comparable to the respective neat polymers. A raise in T_f of both nanocomposites is noticed at higher weight loss temperatures. There is a rise in T_f of 98 °C for CB@PP compared with neat PP resin. An increase in T_f of 92 °C is noticed for CB@PA-6 compared with neat PA-6. The residual weight (R_f) is observed to be greater for CB@PP nanocomposite compared with CB@PA-6. The graphic illustration of the comparison of residual weights at final degradation is presented in figure 4.

Literature is available on properties enhancement by filler addition using physical and chemical interactions. The physical interaction involves the physical modification of the matrix due to reinforcement influences. It supposes that some kind of state of bonding is developed among matrix and carbon black whose exact nature is undefined. The second chemical consideration relies on the surface chemistry of the polymer and carbon black filler. It also works to explain the correlations between the category and the number of linkages and reinforcement outcomes. Usually, C-C or C-H weak interactions are proposed. In most recent studies emphasis is made on the physical modes of interactions [24]. So, baes on these interactions it was concluded that the CB of the bamboo plant has influenced the thermal stability of PP polymers more effectively compared with PA-6 polymer.

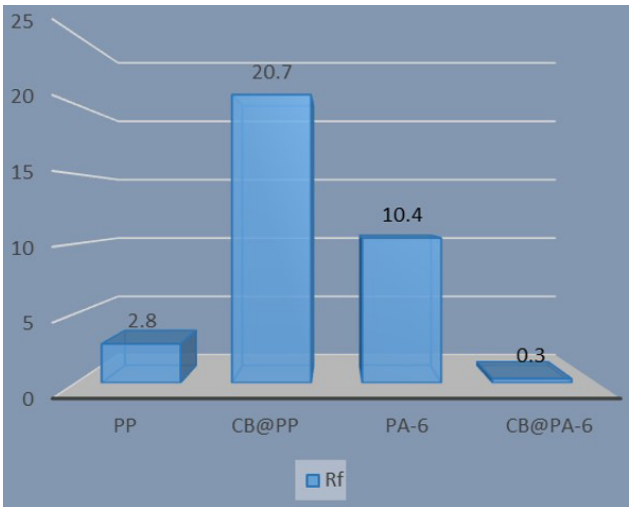

Figure 4: Graphic illustration of thermal stability of nanocomposites in terms of residual weight loss.

Table 4: Melting peaks position from DSC.

Compounds	PP	CB@PP	PA-6	CB@PA-6
T_m (°C)	127.7	126.3	215.2	221.5
H_m (J/g)	174.9	120.3	80.5	57.5

DSC analysis of the samples

Comparative DSC plots of coagulation-processed nanocomposite PP, CB@ PP, PA-6, and CB@PA-6 were investigated over the temperature range of 50 °C to 400 °C. The DSC curves are displayed in figure 5. All the neat polymers and their respective nanocomposites presented an endothermic peak with a very small difference in the value of melting temperature (T_m). There is observed a fall of 1 °C for CB@PP and a 6 °C rise in melting temperature of CB@PA-6 compared with their respective neat polymers. It was noticed that for CB@PA-6 splitting in the melting peak is observed. The obtained data are presented in table 4 for the melting peaks (T_m) and magnitude of the heat of melting.

Conclusions

CB@PP and CB@PA-6 nanocomposites were prepared using the coagulation method. The structural confirmation was achieved by FTIR. It was revealed that mixing CB of the bamboo plant could modify the thermal and melting properties of the neat polymers. The filler has revealed different trends of properties in the selected thermoplastic polymers. CB has enhanced the thermal stability of PP which is assumed to be superior interaction of filler with the aliphatic nonpolar skeleton. PA-6 initially behaved differently because it already contains polar bonds in the polymer skeleton. The lack of effective incorporation of filler into the PA-6 backbone has resulted in a decline in thermal stability for the initial

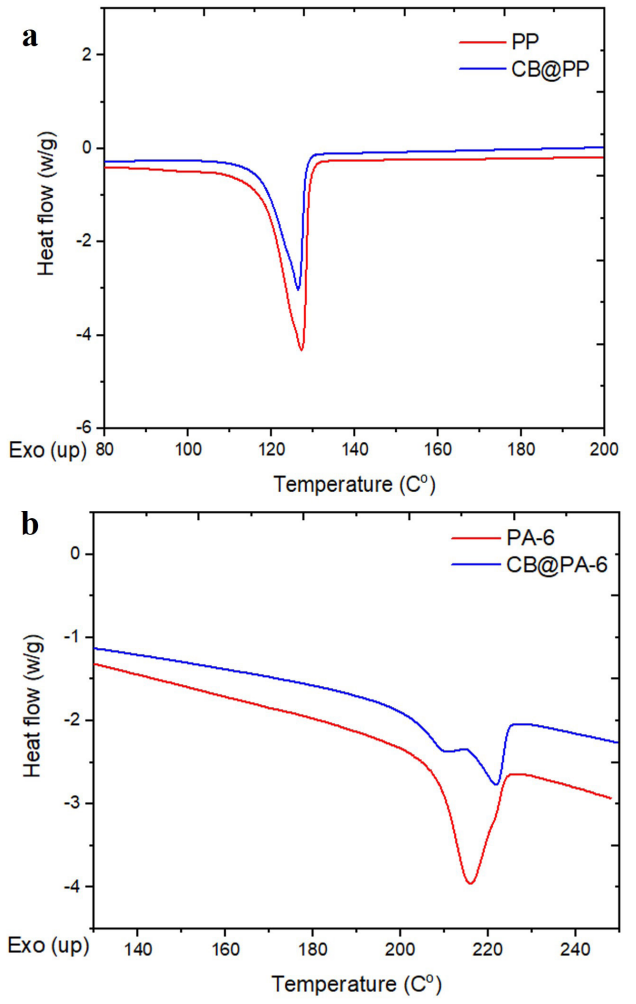

Figure 5: DSC curves of **(a)** PP and CB@PP, and **(b)** PA-6 and CB@PA-6.

weight losses. For higher and final weight loss temperatures the results are comparable to the corresponding neat polymers. DSC analysis predicted the lowering of the heat of melting values of two nanocomposites compared with respective neat polymers. This behavior supports the introduction of tailorable characters in the polymer resin, which is favorable for improving mechanical properties. Thus, the current approach favors the facile fabrication of thermally resistant nanocomposites for the PP using selected filler content compared with PA-6 at initial weight loss. For higher weight loss the thermal stability of both the synthesized nanocomposites showed enhancement as compared with neat thermoplastic polymers.

Acknowledgments

Department of Fundamental and Applied Sciences, Universiti Teknologi PETRONAS (UTP) is greatly acknowledged for this research.

Conflict of Interest

None

References

1. da Silva EL, Torres M, Portugau P, Cuña A. 2021. High surface activated carbon obtained from Uruguayan rice husk wastes for supercapacitor electrode applications: correlation between physicochemical and electrochemical properties. J Energy Storage 44: 103494. https://doi.org/10.1016/j.est.2021.103494
2. Ayub S, Guan BH, Ahmad F. 2020. Graphene and Iron based composites as EMI shielding: A Systematic Review. In Second International Sustainability and Resilience Conference: Technology and Innovation in Building Designs, Sakheer, Bahrain.
3. Bhattarai RM, Chhetri K, Natarajan S, Saud S, Kim SJ, et al. 2022. Activated carbon derived from cherry flower biowaste with a self-doped heteroatom and large specific surface area for supercapacitor and sodium-ion battery applications. Chemosphere 303: 135290. https://doi.org/10.1016/j.chemosphere.2022.135290
4. Ayub S, Guan BH, Ahmad F, Oluwatobi YA, Nisa ZU, et al. 2021. Graphene and iron reinforced polymer composite electromagnetic shielding applications: a review. Polymers 13(15): 2580. https://doi.org/10.3390/polym13152580
5. Nisa ZU, Chuan LK, Ayub S, Guan BH, Ahmad F. 2021. Thermal and morphological characterization of coagulation-processed nanocomposite of polypropylene and bio-nanocarbon obtained from bamboo. In Third International Sustainability and Resilience Conference: Climate Change, Sakheer, Bahrain.
6. Yan B, Feng L, Zheng J, Zhang Q, Jiang S, et al. 2022. High performance supercapacitors based on wood-derived thick carbon electrodes synthesized via green activation process. Inorg Chem Front 9(23), 6108-6123. https://doi.org/10.1039/d2qi01914k
7. Ozpinar P, Dogan C, Demiral H, Morali U, Erol S, et al. 2022. Activated carbons prepared from hazelnut shell waste by phosphoric acid activation for supercapacitor electrode applications and comprehensive electrochemical analysis. Renew Energy 189: 535-548. https://doi.org/10.1016/j.renene.2022.02.126
8. Parra JB, Sousa JD, Bansal RC, Pis JJ, Pajares JA. 1995. Characterization of activated carbons by the BET equation—an alternative approach. Adsorpt Sci Technol 12(1): 51-66. https://doi.org/10.1177/026361749501200106
9. Nisa ZU, Chuan LK, Guan BH, Ahmad F, Ayub S. 2023. Experimental correlation of the role of synthesized biochar on thermal, morphological, and crystalline properties of coagulation processed poly (1, 4-phenylene sulfide) nanocomposites. Polymers 15(8): 1851. https://doi.org/10.3390/polym15081851
10. Boundzanga HM, Cagnon B, Roulet M, de Persis S, Vautrin-Ul C, et al. 2020. Contributions of hemicellulose, cellulose, and lignin to the mass and the porous characteristics of activated carbons produced from biomass residues by phosphoric acid activation. Biomass Conv Bioref 12: 3081-3096. https://doi.org/10.1007/s13399-020-00816-9
11. Yaashikaa PR, Kumar PS, Varjani SJ, Saravanan A. 2019. Advances in production and application of biochar from lignocellulosic feedstocks for remediation of environmental pollutants. Bioresour Technol 292: 122030. https://doi.org/10.1016/j.biortech.2019.122030
12. Park SJ, Seo MK, Nah C. 2005. Influence of surface characteristics of carbon blacks on cure and mechanical behaviors of rubber matrix compoundings. J Colloid Interface Sci 291(1): 229-235. https://doi.org/10.1016/j.jcis.2005.04.103
13. Stoeckli HF. 1990. Microporous carbons and their characterization: the present state of the art. Carbon 28(1): 1-6. https://doi.org/10.1016/0008-6223(90)90086-E
14. Fu Q, Xu W, Li D, Li N, Niu D, et al. 2021. Dynamic compressive behaviour of hybrid basalt-polypropylene fibre-reinforced concrete under confining pressure: experimental characterisation and strength criterion. Cem Concr Compos 118: 103954. https://doi.org/10.1016/j.cemconcomp.2021.103954

15. Chernets MV, Shil'ko SV, Pashechko MI, Barshch M. 2018. Wear resistance of glass-and carbon-filled polyamide composites for metal-polymer gears. J Frict Wear 39: 361-364. https://doi.org/10.3103/S1068366618050069

16. Kausar A. 2019. Advances in carbon fiber reinforced polyamide-based composite materials. Adv Mater Sci 19(4): 67-82. https://doi.org/10.2478/adms-2019-0023

17. Kutz M. 2011. Applied Plastics Engineering Handbook: Processing and Materials. William Andrew.

18. Nisa ZU, Chuan LK, Guan BH, Ayub S, Ahmad F. 2022. Anti-wear and anti-erosive properties of polymers and their hybrid composites: a critical review of findings and needs. Nanomaterials 12(13): 2194. https://doi.org/10.3390/nano12132194

19. Saba N, Md Tahir P, Jawaid M. 2014. A review on potentiality of nano filler/natural fiber filled polymer hybrid composites. Polymers 6(8): 2247-2273. https://doi.org/10.3390/polym6082247

20. Wu Q, Qu B. 2001. Synergistic effects of silicotungistic acid on intumescent flame-retardant polypropylene. Polym Degrad Stab 74(2): 255-261. https://doi.org/10.1016/S0141-3910(01)00155-0

21. Sabaruddin FA, Paridah MT, Sapuan SM, Ilyas RA, Lee SH, et al. 2020. The effects of unbleached and bleached nanocellulose on the thermal and flammability of polypropylene-reinforced kenaf core hybrid polymer bionanocomposites. Polymers 13(1): 116. https://doi.org/10.3390/polym13010116

22. Zhao W, Kundu CK, Li Z, Li X, Zhang Z. 2021. Flame retardant treatments for polypropylene: strategies and recent advances. Compos Part A Appl Sci Manuf 145: 106382. https://doi.org/10.1016/j.compositesa.2021.106382

23. Wilke LA, Robertson CG, Karsten DA, Hardman NJ. 2023. Detailed understanding of the carbon black–polymer interface in filled rubber composites. Carbon 201: 520-528. https://doi.org/10.1016/j.carbon.2022.09.032

24. Kraus G. 2005. Reinforcement of Elastomers by Carbon Black. In Cantow HJ, Dall'Asta G, Ferry JD, Fujita H, Kern W, etal. (eds) Advances in Polymer Science: Fortschritte der Hochpolymeren-Forschung. Springer Berlin, Heidelberg, pp 155-237.